Lithos 190–191 (2014) 264–278

Contents lists available at ScienceDirect

Lithos

journal homepage: www.elsevier.com/locate/lithos

AFC3D: A 3D graphical tool to model assimilation and fractional crystallization with and without recharge in the R environment

Silvina Guzmán [a,*], Roberto Carniel [b,c,d], Pablo J. Caffe [e,f]

[a] IBIGEO—(CONICET-UNSa) Museo de Ciencias Naturales, Universidad Nacional de Salta, Mendoza 2, 4400 Salta, Argentina
[b] Laboratorio di misure e trattamento dei segnali, Dipartimento Ingegneria Civile e Architettura (DICA) Università di Udine, Via delle Scienze, 206-33100 Udine, Friuli, Italy
[c] CICTERRA Facultad de Ciencias Exactas, Físicas y Naturales, Universidad Nacional de Córdoba, Av. Vélez Sarsfield 1611, X5016GCA Córdoba, Argentina
[d] Geognosis Proj., Int. Syst. Lab, National Research University of Information Technologies, Mechanics and Optics, Kronverksky Prospect, 49, St. Petersburg 197101, Russia
[e] CIT Jujuy, Universidad Nacional de Jujuy—CONICET, Avda. Bolivia 1661, San Salvador de Jujuy, Argentina
[f] Instituto de Geología y Minería, Avda. Bolivia 1661, San Salvador de Jujuy, Argentina

ARTICLE INFO

Article history:
Received 11 July 2013
Accepted 5 December 2013
Available online 16 December 2013

Keywords:
Assimilation and fractional crystallization (AFC)
Magma recharge (AFC-r)
Geochemical modeling

ABSTRACT

AFC3D is an original graphical free software developed in the framework of the R scientific environment and dedicated to the modelling of assimilation and fractional crystallization without (AFC) and with (AFC-r) recharge, facilitating the search for the solutions of the equations originally proposed by DePaolo (1981, 1985) and first solved in a graphical way by Aitcheson and Forrest (1994). The software presented here allows a graphical 3D representation of ρ (mass of assimilated crust/mass of original magma) as a function of r (rate of crustal assimilation/rate of fractional crystallization) and β (recharge rate of magma replenishment / rate of assimilation) for each element/isotope, finding a coherent set of (r, β, ρ) parameter triples in a mostly automated way. Mathematically optimized solutions are derived, which can and should then be discussed and evaluated from a geological and petrological point of view by the end user. The presented contribution presents the software and a series of models published in the literature, which are discussed as case studies of application and whose solutions are sometimes enhanced based on the results provided by the software.

1. Introduction

The present paper presents a new free software, AFC3D, dedicated to the modelling of assimilation and fractional crystallization without (AFC) and with (AFC-r) recharge, further developing the graphical solution described by Aitcheson and Forrest (1994) on the base of the formulas originally proposed by DePaolo (1981). The new software approach presented here allows finding a coherent set of r (rate of crustal assimilation / rate of fractional crystallization), β (recharge rate of magma replenishment / rate of assimilation) and ρ (mass of assimilated crust / mass of original magma) parameters in a mostly automated way, based on the analysis of 3D graphical plots. Table 1 summarizes the notations used in the paper.

AFC processes were first envisaged by Bowen (1928), but the first formulas that attempted their modelling were proposed by O'Hara (1977), who considered also discrete, periodical magma replenishments, leading to an iterative computation in which the magma evolution is modelled cyclically. DePaolo (1981) presented formulas to reproduce simultaneous and continuous assimilation and fractional crystallization (AFC). Hence the isotopic ratio and element concentration of a magma undergoing this process depend on the relative rates of assimilation and fractional crystallization (r), the bulk distribution coefficient of the element (D) in the parental magma, the fraction of magma remaining (F) and the element abundance and isotopic composition in the assimilated material (wall rock) and the original magma at a given time. DePaolo (1985) extended these equations for the case of simultaneous recharge in an AFC system, i.e. AFC-r. A significant step forward was then achieved by Aitcheson and Forrest (1994), whose most important contribution was the modification of DePaolo's equations to be able to quantify accurately the crustal contribution during AFC, which was not possible to constrain with the original DePaolo's formulation. For this, the isotopic composition and element concentration in the contaminant and in the original magma, as well as the bulk partition coefficient (D) value must be known. The method proposed by Aitcheson and Forrest (1994) is based on a graphical solution to find optimal r and ρ parameters. The procedure consists in plotting ρ as a function of r for different elements. As the parameters should be theoretically unique, the intersection of the curves corresponding to the different elements gives the most plausible values of r and, consequently, of ρ. In order for this estimation to be sufficiently reliable and produce estimates of r with little uncertainty, one important requirement is that these curves have moderate to high intersection angles. On the contrary, a low intersection angle implies that, taking into account the uncertainties in the input parameters, a wider range of values of r can satisfy the intersection requirements.

* Corresponding author. Tel.: +54 3874212766; fax: +54 3874318086.
E-mail addresses: sguzman@conicet.gov.ar (S. Guzmán), roberto.carniel@uniud.it (R. Carniel), pabcaffe@idgym.unju.edu.ar (P.J. Caffe).

0024-4937/$ – see front matter © 2013 Elsevier B.V. All rights reserved.
http://dx.doi.org/10.1016/j.lithos.2013.12.005

Table 1
The main notations used in the paper.

C_a	Element concentration in the wall-rock melt
C^*_m	Element concentration in the original magma (which is also used also as the recharge magma)
C_m	Element concentration in the contaminated magma
ε_a	Isotopic ratio in the wall-rock melt
ε_m	Isotopic composition of assimilated igneous rock
ε^*_m	Isotopic ratio in original magma
D	Bulk partition coefficient*
M_a	Mass of assimilated crust
M^o_m	Mass of original magma
M_r	Mass of recharge magma
M_c	Mass of crystals effectively separated from the magma
M_m	Mass of remaining crystals (including neutrally buoyant ones)
$\dot{M}_a$	Rate of assimilation
$\dot{M}_c$	Rate of crystallization
$\dot{M}_r$	Rate of replenishment
ρ	Mass of assimilated crust/mass of original magma
β	Rate of magma replenishment/rate of assimilation; $\beta = \dot{M}_r/\dot{M}_a$
r	Rate of assimilation of crust/rate of fractional crystallization; $r = \dot{M}_a/\dot{M}_c$
F	mass of magma remaining
% of crustal assimilation	$=(\rho / (\rho + 1))^*100$
$r^*\beta$	$=\dot{M}_r/\dot{M}_c$
λ	$=(\varepsilon^o_m - \varepsilon_m) / (\varepsilon_m - \varepsilon_a)$
γ	$=C_a / C^o_m$

* The bulk partition coefficient (D) for a given element (e.g. Sr) can be computed as follows: $D_{Sr} = (\text{Mineral}_1\ \text{vol.\%} * Kd^{Sr}{}_{\text{mineral 1}}) + (\text{Mineral}_2\ \text{vol.\%} * Kd^{Sr}{}_{\text{mineral 2}}) + \ldots. + (\text{Mineral}_n\ \text{vol\%} * Kd^{Sr}{}_{\text{mineral n}})$, in which Minerals 1 to n are crystalline phases under fractionation from the original magma.

In the following we will consider only the Aitcheson and Forrest (1994) equations where D and r are constant throughout the whole AFC or AFC-r process. Note that this requirement for a constant r does not necessarily imply constant rates of assimilation or fractional crystallization, but only a constant ratio between them (Aitcheson and Forrest, 1994).

2. AFC without recharge

In the case where no magma recharge is assumed, Eq. [5] from Aitcheson and Forrest (1994) is used to compute ρ as a function of r. This expression is particularly useful when there are many phenocrysts in the contaminated magma, which implies that the C_m (concentration of an element in the contaminated magma) estimate is probably not reliable. In this case, as previously stated by DePaolo (1981), r and D are assumed as (approximately) constant during the whole AFC process. We underline again that a constant r does not necessarily imply constant rates of assimilation or fractional crystallization.

Input parameters needed:

- C_a and ε_a: element concentration and isotopic ratio in the wall-rock melt
- C^o_m and ε^o_m: element concentration and isotopic ratio in the original magma
- D: bulk partition coefficient of the original magma fractionating mineral assemblage
- ε_m: isotopic composition of assimilated igneous rock, that may be represented by a single rock sample, or an average from all rock samples under study.

Restrictions (i.e. cases not allowed): $r + D = 1, r = 1$

Input parameters not needed [enhancement in relation to DePaolo (1981) formulas]:

- F: fraction of magma remaining
- C_m: concentration of the element in the contaminated magma.

The graphical solution is determined by plotting ρ as a function of r for each element. In this way we obtain curves that largely depend on the value of D for any given element. Using as many elements as possible, the (hopefully common) intersection of the curves associated to the different elements determines possible values of ρ and r, as they have to be equal for all elements. Note that at least two elements are needed for this method to be applied. Moreover, for the method to be accurate it is necessary to achieve a high angle of intersection of curves; consequently, elements with widely differing values of D must be used. To find ρ with this procedure, no assumption on the value of r is needed, but the two parameters can be estimated together. In Aitcheson and Forrest (1994), Eq. [5] is well defined and can be used only if the condition $r \geq \lambda(1 - D) / (\gamma + \lambda)$ is satisfied.

In the case in which the C_m value is reliable (i.e. a sample without phenocrysts) or in which few or no isotopic data is available, ρ can be computed from concentrations only, using Aitcheson and Forrest (1994) Eq. [6].

Input parameters needed:

- C_a: element concentration in the wall-rock melt
- C^o_m: element concentration in the original magma
- C_m: element concentration in the contaminated magma
- D: bulk partition coefficient of the original magma fractionating mineral assemblage.

Another way to find ρ is using Aitcheson and Forrest (1994) Eq. [7]. In this case the input data include concentrations and isotopes of all magmas (original, assimilated and contaminated magma) excluding the C_a data. This approach should be used when C_a estimate is not considered very reliable. On the contrary, Eq. [6] is preferred when the ε_a estimate is not reliable.

Aitcheson and Forrest (1994) recommend the use of minimum and maximum values for all the parameters (the way of choosing maximum and minimum parameters comes in Table 1 of that paper, which we reproduce here as Table 2) thus obtaining an area of overlapping that finally gives possible values of ρ as a function of r. These can be applied for all equations of the non-recharge situation (Eqs. [5], [6] and [7]) and also for equations of the recharge situation (Eqs. [9], [10] and [11]; see later in the text).

3. AFC with magma recharge

The assimilation and fractional crystallization can occur with the addition of fresh magma to the system (open system). These equations are based on the fact that the amount of crust that can be assimilated is

Table 2
Parameter replacement for the computation of the minimum and maximum possible values of ρ.

Parameter	Maximum ρ	Minimum ρ
In all cases		
D is replaced by	Minimum D	Maximum D
Ca is replaced by	Minimum C_a	Maximum C_a
Com is replaced by	Maximum C^o_m	Minimum C^o_m
For $\varepsilon_a > \varepsilon^o_m$ (usually Sr and O, sometimes Pb)		
ε_a is replaced by	Minimum ε_a	Maximum ε_a
ε^o_m is replaced by	Maximum ε^o_m	Minimum ε^o_m
ε_m is replaced by	Maximum ε_m	Minimum ε_m
For $\varepsilon_a < \varepsilon^o_m$ (usually Nd, sometimes Pb)		
ε_a is replaced by	Maximum ε_a	Minimum ε_a
ε^o_m is replaced by	Minimum ε^o_m	Maximum ε^o_m
ε_m is replaced by	Minimum ε_m	Maximum ε_m
For $C_a > C^o_m$ (e.g. Nd, Pb)		
C_m is replaced by	Maximum C_m	Minimum C_m
For $C_a < C^o_m$ (e.g. Sr)		
C_m is replaced by	Minimum C_m	Maximum C_m

related to the amount of heat that is supplied to the system. Previous works (e.g., DePaolo, 1985; Reagan et al., 1987) have proposed equations to model AFC-r but failed in quantifying the crustal component. The equations of Aitcheson and Forrest (1994) do not assume constant rates of recharge and assimilation during the time in which magma is crystallizing, but only a constant ratio (r) between these rates, during the whole process, so these equations can be used for both the cases of periodic and continuous replenishment. For the scope of this program, and given the logical uncertainties of modelling AFC-r processes, we have simplified the formulas given by Aitcheson and Forrest (1994), assuming that the recharge magma is the same as the original magma.

Aitcheson and Forrest (1994) use Eqs. [10] and [11] for the AFC-r to obtain an auxiliary parameter [$\rho' = (M_r + M_a) / M^o{}_m$], which then can be substituted in Eq. [9] to obtain ρ (crust/magma ratio) in recharge situations ($\rho_r = M_a / (M^o{}_m + M_r)$; where M_a: mass of wall-rock magma, $M^o{}_m$: mass of original magma, and M_r: mass of recharge magma).

It should be noted that AFC-r Eq. [10] (recharge situation) is equivalent to AFC Eq. [5] (non-recharge situation) that need to use isotope data and that AFC-r Eq. [11] (recharge situation) is equivalent to AFC Eq. [6] (non-recharge situation). Thus, the input parameters needed are the same for the recharge and non-recharge situations, as the recharge and original magmas are considered to be the same.

As suggested by Aitcheson and Forrest (1994), with the AFC3D software we can plot the data of both equations in the same diagram, then enhancing the reliability of the resulting models. As will be seen later in the examples of the application section, the software also allows the user to choose the elements/isotopes that best fit a common modelling, i.e. using only the data that make the results more reliable by choosing the ones that lead to a higher intersection angle and a more precise common intersection.

Input parameters needed for Eq. [10] and [9]:

- C_a and ε_a: element concentration and isotopic ratio in the wall-rock melt
- C^o_m and ε^o_m: element concentration and isotopic ratio in the original magma (here considered the same as the recharge magma, i.e. C_r and ε_r).
- D: bulk partition coefficient of the original magma fractionating mineral assemblage
- ε_m: isotopic composition of assimilated igneous rock, that can come from a single sample of the rocks under study or be their average.

Input parameters needed for Eqs. [11] and [9]:

- C_a: element concentration in the wall-rock melt
- C^o_m: element concentration in the original magma (here considered the same as the recharge magma, i.e., C_r)
- C_m: element concentration in the contaminated magma
- D: bulk partition coefficient of the original magma fractionating mineral assemblage.

When ρ is plotted as a function of r and β for several elements, a surface for each element is created. Then the intersection of the surfaces gives an estimate of the values of ρ_r, r and β with no previous assumptions.

As for pure AFC, the AFC-r case yields a ρ_r value that is estimated as a function of r and β in a procedure similar to the one described above, where the maximum and minimum parameters can be chosen using Table 2. Aitcheson and Forrest (1994) show also some formulae to find restrictions on the admissible values of r. The software presented here automatically carries out verification of these restrictions.

4. AFC3D program features

The software presented here enhances the tools given by the graphical method of Aitcheson and Forrest (1994), implementing their Eqs. [5], [6], [7], [9], [10] and [11]. With this program the user can graphically model AFC and AFC-r and easily obtain the graphs given in Aitcheson and Forrest (1994) to find the best estimates for r and ρ. As mentioned above, an additional feature of the AFC3D software is the fact that the user does not need verification of any restrictions on the value of the parameters, as the program calculates automatically the restrictions e.g. on the admissible r values in Eqs. [5] and [10] of Aitcheson and Forrest (1994).

Moreover, a new 3D representation is proposed, showing ρ as a function of both r and β for the AFC-r case. Surfaces are drawn for each element and their intersection can be determined in a graphical way, like in Aitcheson and Forrest (1994), but in 3D, thus avoiding the long trial-and-error procedure needed to determine both r and β with their method. The coordinates (r, β, ρ) of these intersection points in the 3D graphs can be also determined numerically by fixing a threshold (zero_threshold) for automatically computing and accepting an intersection. In other words, the difference between all ρ values for the selected element set (which should be theoretically zero, as they should all coincide) cannot exceed the given threshold: zero_threshold. This is a numerical compromise that has to be accepted in order to find solutions. If this threshold is fixed too low, the software will give a warning that no intersections are found, and the user will have to raise its value. If, in order to obtain some intersections, the required threshold is relatively high, the user should evaluate the possibility of eliminating the element that produces a value of ρ that departs most from the others. The optimal threshold value can slightly change with the number of points into which the r and β range are divided. Obviously, choosing a sufficiently high value for the threshold always leads to a set of solutions, but these could become not very reasonable. Therefore, although there is no strict rule, we recommend to be very careful when thresholds exceed values of about 1E−2. Sometimes the calculations of the formulas for some specific pair or r and β values can lead to numerical instabilities and corresponding anomalous solutions which appear as spikes in the output graphs. If this happens, it is usually easy to remove them by slightly changing the number of points into which r and β ranges are divided, e.g., from 200 to 209 points.

The solution is of course almost never unique, and often a full set of points belonging to a curve are all potential solutions of the model. Actually, Roberts and Clemens (1995) pointed out that having such powerful mathematical formalisms can lead to viable petrogenetic models for essentially any group of related rocks, even those unconstrained by either geological or major-element geochemical data. The evaluation of the geological and petrological plausibility of the different solutions remains therefore the responsibility of the researcher, and the software cannot provide any control on that. However, three "potentially best" solutions in a mathematical sense are determined and proposed by the software. The first solution is determined as follows: the average β is computed among all the β solutions; the closest β among the solutions listed to this average value is determined; the corresponding r and ρ are finally determined. The second solution is determined in an analogous way, but working on the r parameter: the average r is computed among all the r solutions; the closest r to this value is determined among the solutions listed; the corresponding β and ρ are finally determined. This second solution is usually less appropriate than the first, because usually β has a greater dispersion with respect to r, and therefore many different β can be used with a single or very similar values of r. Finally, the third proposed solution is determined by seeking the minimum dispersion between the differences in ρ among all the couple of possible elements. This solution represents somehow the best mathematical approximation of a real intersection among all the elements and represents therefore probably the most reasonable solution. Moreover, the user can also choose the result from the whole set, considering the one that she/he considers best fits the geological and petrological evidences.

Once a solution is chosen graphically or numerically based on the 3D graphs, the corresponding values of β and r can be fixed and 2D graphs similar to Fig. 4a and b of Aitcheson and Forrest (1994) can be plotted,

which represent 2D slices of the 3D plot parallel to the r and β axis respectively.

The program can highlight also solutions with $\beta = 0$, which suggest that a non-recharge solution is more plausible than a solution with recharge. This is the case e.g. for Lille Kufjord intrusions (see examples of application in the input data file). In these cases, the user can examine the graph corresponding to Fig. 1 and 2 of Aitcheson and Forrest (1994) that are calculated with Eqs. [5] and [6] of Aitcheson and Forrest (1994), which are also produced by the program. For the non-recharge case the program also produces graphs of F as a function of r. This can be done both by using Eq. [4] as proposed by Aitcheson and Forrest (1994) and by inverting their Eq. [3], which has the advantage of being valid for both elements concentrations only and isotopes. All these graphs are also stored as external files.

5. Program execution

The software AFC3D can be freely obtained from the authors by sending a request email, preferably describing the intended use. It consists of three scripts (AFC3D_Install_Packages.R, AFC3D_Main.R and AFC3D_Input_Data.R) all of which have to be copied to a directory of choice (e.g. C:\AFC3D under Windows, or/home/username/AFC3D under Linux).

This software runs within the free R program environment (R Development Core Team, 2012), so the very first step is to install R if not already available on the system. Downloads can be carried out from any of the CRAN mirrors (http://cran.r-project.org/mirrors.html). Supported operating systems are Linux, Max OS X and Windows. Moreover, R is available as part of many Linux distributions, so the user should check first within their distribution software manager, and download it from CRAN only if not available there.

Once R is installed, it can be executed. This is done in Linux by giving the command R in a terminal window, in Windows by clicking the corresponding program icon on the desktop. In Windows it is suggested to modify the properties of the icon to start the program from the same directory where the AFC3D scripts have been copied (e.g. C:\AFC3D). In a similar way, also in Linux the user should change the current directory to that directory before executing R. Once R is executed, the R prompt is obtained:

```
>
```

The next step is to install the R packages that are needed to run the AFC3D program.

```
> source ('AFC3D_Install_Packages.R')
```

An internet connection is still required at this stage, and R asks to choose the preferred (closest and/or fastest) CRAN mirror. Reasonably it is good to choose a mirror from your own country.

The packages that are needed and installed automatically by this script are Hmisc (Harrell, 2012) and rgl (Adler and Murdoch, 2012).

This package installation has to be carried out only once on each system, although it is suggested to do it again after a possible future upgrade of the R environment.

To run the main script of the program AFC3D, the following command should be entered at the R prompt. This has to be done every time one wants to execute the software.

```
> source ('AFC3D_Main.R')
```

This script automatically loads the file AFC3D_Input_Data.R which has to reside in the same directory and contains the input parameters, both from the given examples and those possibly inserted by the user. The user is advised not to change the name of this file. However, he/she is advised to make backup copies of the AFC3D_Input_Data.R before modifying it for new experiments.

For users that do not feel confident with R syntax and/or have to input a considerable number of element/isotope data, an alternative way of specifying element/isotope input data is provided, i.e. by using a common spreadsheet in the same folder, that can be modified in Microsoft Excel, LibreOffice, OpenOffice or similar programs, and saved in the common CSV (comma separated values) format. The spreadsheet is named AFC3D_InputData.csv and will also be automatically read by the program AFC3D_Main.R. The user is only advised to number the elements/isotopes exclusively, as elements/isotopes defined in the spreadsheet and in the AFC3D_Input_Data.R will be all merged together, with AFC3D_Input_Data.R definitions overriding the ones with the same element/isotope identifier number in the spreadsheet. As a side effect, this can be useful for making rapid tests on the influence of small variations of an element/isotope parameter by modifying the AFC3D_Input_Data.R without modifying the "real" data in the spreadsheet.

Let's make a pause here to learn in detail how to work with the input data for then returning to the program execution

5.1. Input data management

A file named AFC_Input_Data.R is included with the program script files. This is the only file that the user is required to modify and work with.

The first paragraphs within this file are comments that describe how to use the file.

A set of predefined examples follow, giving the user a more concrete idea on how to implement his/her own modelling.

In the R script language when # is present at the beginning of a line, the entire line is considered a comment, so that none of this information is used in the calculations. Conversely, when the line begins with no # symbol (see Fig. 1), the data is used for calculations. This allows the user to uncomment a single line at a time, executing one and only one of the provided examples without the need to delete the others from the file.

To maintain the input file as easy to read, each example makes reference to a set of elements, whose features are described in a different section of the AFC_Input_Data.R file. This also allows to list different, possibly alternative variants of examples using the same set of elements.

To include a new, personal model the user needs first to add the elements and isotopes of her/his case of study to the input data file. As can be seen in the AFC3D_input data.R file, each element is given in square brackets; the examples given are numbered always in a way that makes the user distinguish elements from each example. A suggested way is as follows: example 1 begins with 1, example 2 with 21, example 3 with 31, etc. This is absolutely not compulsory, but it allows successive insertion of new elements and keeps the input file cleaner. We can then decide which Aitcheson and Forrest (1994) equations we are going to use. As we previously said for AFC-r we can use Eqs. [10] and [9] when isotopes are available; in this case the line below the definition of each element has to set Concentrations_Only[, No_of_El] = 0.

On the contrary, if we select and set Concentrations_Only[, No_of_El] = 1 the program will automatically work with Eqs. [11] ans [9] because no isotopic data are available.

Let's reproduce the example of AFC-r given in Aitcheson and Forrest (1994) for the central volcanic zone lavas. We then need to erase the # symbol at the beginning of the line that contains this information (see Fig. 1). Note that this example only uses isotopic data. For this reason the Concentrations_Only[,No_of_El] for each element is always equal to 0. We numbered the elements as follows (see Fig. 2):

[21] for $^{87}Sr/^{86}Sr$
[22] for ε Nd
[23] for $\delta^{18}O$
[24] for $^{206}Pb/^{204}Pb$
[25] for $^{207}Pb/^{204}Pb$
[26] for $^{208}Pb/^{204}Pb$.

```
# For each example one has to define:
# First_Element: First element to use
# Last_Element: Last element to use
# fixed_r: value of r to be used in 2D plots
# fixed_beta: value of beta to be used in 2D plots
# Elements_to_Intersect=c(#1,#2,#3...): list of elements to intersect to get solutions
# zero_threshold: threshold for the distance between points for an intersection to be accepted
#
# Plot limits are used for Fig. 1, Fig. 2, Fig. 4a, Fig. 4b and 3D plots (Device 1 and 2)

# UNCOMMENT ONLY *ONE* example at a time
#

# Examples of application

# Lille Kufjord Sample_Aitcheson and Forrest_1994
# First_Element=1; Last_Element=2; fixed_r = 0.08; fixed_beta = 0.0; Elements_to_Intersect=c(1,2); zero_threshold=2e-4; rlim_min=0.0; rlim_max=0.2;
 r_number_of_points=200; betalim_min=0.0; betalim_max=0.1; beta_number_of_points=200; rholim_min=0.0; rholim_max=0.2; Flim_min=0.0; Flim_max=1;
# First_Element=1; Last_Element=2; fixed_r = 0.08; fixed_beta = 0.0; Elements_to_Intersect=c(1,2); zero_threshold=3.7e-5; rlim_min=0.0; rlim_max=0.2;
 r_number_of_points=200; betalim_min=0.0; betalim_max=0.1; beta_number_of_points=200; rholim_min=0.0; rholim_max=0.2; Flim_min=0.0; Flim_max=1;

# CVZ lavas - Aitcheson and Forrest_1994
# First trial
# First_Element=21; Last_Element=26; fixed_r = 0.2; fixed_beta = 0.9; Elements_to_Intersect=c(21,22,23,24,25,26); zero_threshold=1e-2; rlim_min=0.0;
rlim_max=0.8; r_number_of_points=209; betalim_min=0.0; betalim_max=4.0; beta_number_of_points=209; rholim_min=0.0; rholim_max=0.8; Flim_min=0.0;
Flim_max=1.0;
# Second trial
# First_Element=21; Last_Element=26; fixed_r = 0.15; fixed_beta = 3.2; Elements_to_Intersect=c(21,22,23,24,26); zero_threshold=1e-2; rlim_min=0.0;
rlim_max=0.8; r_number_of_points=209; betalim_min=0.0; betalim_max=4.0; beta_number_of_points=209; rholim_min=0.0; rholim_max=0.8; Flim_min=0.0;
Flim_max=1.0;# Second step
# Third trial
First_Element=21; Last_Element=26; fixed_r = 0.15; fixed_beta = 3.2; Elements_to_Intersect=c(21,22,23,24,26); zero_threshold=83e-4;
rlim_min=0.0; rlim_max=0.4; r_number_of_points=209; betalim_min=0.0; betalim_max=4.0; beta_number_of_points=209; rholim_min=0.0;
 rholim_max=0.3; Flim_min=0.0; Flim_max=1.0;
```

Fig. 1. Part of the input data file where the user sets the ranges and conditions that will be used in the model. In this particular case the model that can be run is the one that lacks the # at the beginning of the line, i.e. the third trial of CVZ lavas.

Although this example has been modelled and published and thus it is easy to reproduce, we provide a set of three trials (we recommend the user to try the first two trials also to understand the influence of changing input parameters), the last one being the one that works properly for the modelling. The information used for this example is seen in Fig. 1, and is as follows:

CVZ lavas—Aitcheson and Forrest, 1994
# Third trial
First_Element = 21; Last_Element = 26; fixed_r = 0.15; fixed_beta = 3.2;
Elements_to_Intersect = c(21,22,23,24,26); zero_threshold = 83E −4; rlim_min = 0.0; rlim_max = 0.4;
r_number_of_points = 209; betalim_min = 0.0; betalim_max = 4.0; beta_number_of_points = 209; rholim_min = 0.0;
rholim_min = 0.0; rholim_max = 0.3; Flim_min = 0.0; Flim_max = 1.0;

It is also important to choose an adequate zero_threshold (if no possible intersection is given we should increase this value, instead if we find too many, or unreasonable, intersections we should lower it). We can also choose the extreme values for r, β, ρ and F respectively; here we have to insert the minimum and maximum reasonable values of each parameter and also the number of points into which each parameter range will be divided (which will become possible results or intersections for r and β in the considered range).

Now we have to enter the values of the elements/isotopes data (D, C_a, C^o_m, etc.) in the corresponding element (see Fig. 2), in this case the values are set for the elements 21, 22, 23, 24, 25 and 26. At the beginning of the row D[,No_of_El] represents the average value of D, D_min[,No_of_El] and D_max[,No_of_El] are the minimum and maximum possible value of D respectively; all these data should be filled by the user when working with their models. When only one D value is available, of course D_min and D_max will coincide with D. The other input data (e.g., C_a, C^o_m, etc.) are filled in a similar way.

In practice, to add our own example we need to copy and paste an existing working example and rewrite it with our own data, so that we are sure the original R syntax of the variable definitions is maintained. We can then include new elements, e.g. numbered [61], [62], etc. It is very important to remember that each time we change the input data we have to save the AFC_Input_Data.R file and execute again the program [> source ('AFC3D_Main.R')] to see the new results.

As mentioned before, the user can alternatively list the elements/isotopes parameters in the spreadsheet AFC3D_InputData.csv. The names of the parameters, listed in the first row of the spreadsheet, are exactly the same as the ones described for the AFC_Input_Data.R file.

Now we are able to proceed with the program execution:

> source ('AFC3D_Main.R')

The R console shows a set of columns (Fig. 3), the first one on the left displays a set of numbers in square brackets (labelled [1,], [2,], etc.) that correspond to the number of solutions given the r, ρ and β range of values in the input data. The second column (labelled [, 1]) correspond to the values of r, the third (labelled [, 2]) to the possible values of β, the fourth (labelled [,3]) to the average values of ρ, the fifth and sixth,...,n (labelled [,4] and [,5]..., [n,]) to the possible values of ρ for a given solution of each of the different variables-elements.

For the CVZ example of Aitcheson and Forrest (1994) results from the different columns are as follows:

[,1] r values
[,2] β values
[,3] average ρ values
[,4] possible ρ values for a given solution for (see Fig. 1, element 21) $^{87}Sr/^{86}Sr$
[,5] possible ρ values for a given solution for (see Fig. 1, element 22) ε Nd

```
## [21]: CVZ lavas - Sr, from Table 3, Aitcheson and Forrest, 1994
No_of_El=21;
Concentrations_Only[,No_of_El]=0;
Elements[,No_of_El]="Sr"
D[,No_of_El] = 0.1000;  D_min[,No_of_El]= 0.02;  D_max[,No_of_El]=0.18;
Ca[,No_of_El] = 150.0000; Ca_min[,No_of_El]= 70.0;  Ca_max[,No_of_El]=230.0;
C0m[,No_of_El] = 300.0000; C0m_min[,No_of_El]= 200.0;  C0m_max[,No_of_El]=400.0;
ea[,No_of_El] = 0.74; ea_min[,No_of_El]= 0.710;  ea_max[,No_of_El]=0.770;
e0m[,No_of_El] = 0.7033; e0m_min[,No_of_El]= 0.7028;  e0m_max[,No_of_El]=0.7038;
em[,No_of_El] = 0.7062; em_min[,No_of_El]= 0.7059;  em_max[,No_of_El]=0.7065;

## [22]: CVZ lavas - Nd, from Table 3, Aitcheson and Forrest, 1994
No_of_El=22;
Concentrations_Only[,No_of_El]=0;
Elements[,No_of_El]="Nd"
D[,No_of_El] = 0.2500;  D_min[,No_of_El]= 0.05;  D_max[,No_of_El]=0.45;
Ca[,No_of_El] = 30.0000; Ca_min[,No_of_El]= 10.0;  Ca_max[,No_of_El]=50.0;
C0m[,No_of_El] = 3.0000; C0m_min[,No_of_El]= 1.0;  C0m_max[,No_of_El]=5.0;
ea[,No_of_El] = -10.0; ea_min[,No_of_El]= -12.0;  ea_max[,No_of_El]=-8.0;
e0m[,No_of_El] = 8.5; e0m_min[,No_of_El]= 7.5;  e0m_max[,No_of_El]=9.5;
em[,No_of_El] = -4; em_min[,No_of_El]= -4.1;  em_max[,No_of_El]=-3.9;

## [23]: CVZ lavas - O, from Table 3, Aitcheson and Forrest, 1994
No_of_El=23;
Concentrations_Only[,No_of_El]=0;
Elements[,No_of_El]="O"
D[,No_of_El] = 1.0;  D_min[,No_of_El]= 0.99;  D_max[,No_of_El]=1.01;
Ca[,No_of_El] = 50.0000; Ca_min[,No_of_El]= 45.0;  Ca_max[,No_of_El]=55.0;
C0m[,No_of_El] = 50.0000; C0m_min[,No_of_El]= 45.0;  C0m_max[,No_of_El]=55.0;
ea[,No_of_El] = 10.0; ea_min[,No_of_El]= 8.0;  ea_max[,No_of_El]=12.0;
e0m[,No_of_El] = 5.7; e0m_min[,No_of_El]= 5.4;  e0m_max[,No_of_El]=6.0;
em[,No_of_El] = 6.7; em_min[,No_of_El]= 6.6;  em_max[,No_of_El]=6.8;

## [24]: CVZ lavas - 206Pb/204Pb, from Table 3, Aitcheson and Forrest, 1994
No_of_El=24;
Concentrations_Only[,No_of_El]=0;
Elements[,No_of_El]="206Pb"
D[,No_of_El] = 0.02;  D_min[,No_of_El]= 0.001;  D_max[,No_of_El]=0.039;
Ca[,No_of_El] = 20.0000; Ca_min[,No_of_El]= 10.0;  Ca_max[,No_of_El]=30.0;
C0m[,No_of_El] = 1.0000; C0m_min[,No_of_El]= 0.1;  C0m_max[,No_of_El]=1.9;
ea[,No_of_El] = 17.6; ea_min[,No_of_El]= 17.1;  ea_max[,No_of_El]=18.1;
e0m[,No_of_El] = 18.7; e0m_min[,No_of_El]= 18.5;  e0m_max[,No_of_El]=18.9;
em[,No_of_El] = 17.85; em_min[,No_of_El]= 17.65;  em_max[,No_of_El]=18.05;

## [25]: CVZ lavas - 207Pb/204Pb, from Table 3, Aitcheson and Forrest, 1994
No_of_El=25;
Concentrations_Only[,No_of_El]=0;
Elements[,No_of_El]="207Pb"
D[,No_of_El] = 0.02;  D_min[,No_of_El]= 0.001;  D_max[,No_of_El]=0.039;
Ca[,No_of_El] = 20.0000; Ca_min[,No_of_El]= 10.0;  Ca_max[,No_of_El]=30.0;
C0m[,No_of_El] = 1.0000; C0m_min[,No_of_El]= 0.1;  C0m_max[,No_of_El]=1.9;
ea[,No_of_El] = 15.62; ea_min[,No_of_El]= 15.54;  ea_max[,No_of_El]=15.70;
e0m[,No_of_El] = 15.615; e0m_min[,No_of_El]= 15.58;  e0m_max[,No_of_El]=15.65;
em[,No_of_El] = 15.619; em_min[,No_of_El]= 15.59;  em_max[,No_of_El]=15.65;

## [26]: CVZ lavas - 208Pb/204Pb, from Table 3, Aitcheson and Forrest, 1994
No_of_El=26;
Concentrations_Only[,No_of_El]=0;
Elements[,No_of_El]="208Pb"
D[,No_of_El] = 0.02;  D_min[,No_of_El]= 0.001;  D_max[,No_of_El]=0.039;
Ca[,No_of_El] = 20.0000; Ca_min[,No_of_El]= 10.0;  Ca_max[,No_of_El]=30.0;
C0m[,No_of_El] = 1.0000; C0m_min[,No_of_El]= 0.1;  C0m_max[,No_of_El]=1.9;
ea[,No_of_El] = 38.10; ea_min[,No_of_El]= 37.1;  ea_max[,No_of_El]=39.1;
e0m[,No_of_El] = 38.65; e0m_min[,No_of_El]= 38.3;  e0m_max[,No_of_El]=38.8;
em[,No_of_El] = 38.23; em_min[,No_of_El]= 37.73;  em_max[,No_of_El]=38.73;
```

Fig. 2. Part of the input data file where the user enters the parameters of each element/isotope ratio. In this particular case, elements that are shown are those used for the CVZ lavas example of Aitcheson and Forrest (1994).

```
          [,1]      [,2]      [,3]      [,4]      [,5]      [,6]      [,7]      [,8]
[1,] 0.1511962 2.985646 0.1626790 0.1587090 0.1669415 0.1617142 0.1670035 0.1590269
[2,] 0.1511962 3.004785 0.1627851 0.1587228 0.1669848 0.1621821 0.1670061 0.1590294
[3,] 0.1511962 3.023923 0.1628952 0.1587367 0.1670285 0.1626700 0.1670088 0.1590320
[1] "solution from average beta:"
[1] 0.1511962 3.0047847 0.1627851
[1] "solution from average r:"
[1] 0.1511962 2.9856459 0.1626790
[1] "solution from minimum variance:"
[1] 0.1511962 3.0239234 0.1628952
[1] 21    Sr      beta <    5.82758620689651
[5]  r >  0.131818181818183
[1] 22    Nd      beta <    4.8
[5]  r >  0.129310344827586
[1] 23    O       beta <  3.3    r >  0
[1] 24    206Pb   beta <    5.88235294117649
[5]  r >  0.142393162393162
[1] 25    207Pb   beta <    4.99999999999778
[5]  r >  0.163333333333394
[1] 26    208Pb   beta <    6.19047619047595
[5]  r >  0.136291390728481
>
```

Fig. 3. Output results of AFC3D found in the R console. The possible intersections of the different elements/isotope ratios give a set of solutions for r, β and ρ for the CVZ lavas example of Aitcheson and Forrest (1994). The box shows three suggested solutions, see text for further details.

[,6] possible ρ values for a given solution for (see Fig. 1, element 23) $\delta^{18}O$

[,7] possible ρ values for a given solution for (see Fig. 1., element 24) $^{206}Pb/^{204}Pb$

[,8] possible ρ values for a given solution for (see Fig. 1., element 26) $^{208}Pb/^{204}Pb$.

If more elements are considered, the successive columns should correspond to other elements/isotopes.

[,n] possible ρ values for a given solution for a given (x) element/isotope.

The results of the example are shown in Fig. 3. In the lower part of the window (see box in Fig. 3) three suggested solutions are shown: i) solution from average β, it has three columns that correspond to r, β and ρ; in a similar way there is ii) solution from average r, and finally iii) solution from minimum variance (with β and r values that minimize the total error). The last lines are restrictions for each element that are computed automatically following Aitcheson and Forrest (1994).

A set of graphics are represented in different windows, they coincide with those presented in Aitcheson and Forrest (1994) and we left their numbers unchanged (see Fig. 4a–d). New graphs developed with AFC3D software are 3D and enable to find the intersections of the surfaces developed by each element/isotope (see Fig. 4e–f):

The user is recommended to run trial 1 of CVZ lavas that indicates the need of avoiding the use of element [25], i.e. $^{207}Pb/^{204}Pb$ for the intersections; it may be also useful to run trial 2 of CVZ lavas, for which a set of 70 solutions is provided. After this step the possible range of the different parameters can be reduced and also the threshold (see trial 3 of CVZ). This is performed by choosing the extreme values for r, β and ρ based on the solutions provided by the program. Thus we have to modify the AFC3D_Input_data.R file with the extreme values that the program has given in the previous step. It is noteworthy that if we reduce the range of each parameter and maintain constant the number of points into which this range is divided, we obtain more accurate results because the distribution of such points will be denser (see trial 3 of CVZ). Output RGL device 1 or RGL device 2 figures are 3D graphs. Clicking on them and moving the mouse enables the user to have different points of view of the cube and better explore the intersections between the different surfaces (defined by each element/isotope). The observation of the intersections (graphically or numerically derived) enable then the user to select fixed r and fixed β values and produce 2D figures. In the style of Figs. 4a and b of Aitcheson and Forrest (1994), which are conceptually 2D cross sections parallel to the r and β axes, that again should show clearly the intersections. Note that for this example, in Fig. 2 of Aitcheson and Forrest (1994), i.e., Fig. 4b (this work), the lines representing the upper bound of most of the elements are lacking. This is because for such extreme values of the parameters, the only admitted solutions imply $\beta > 0$ (recharge).

When we consider the detected solution sufficiently reliable, this will consist in a set of output parameters that are r, β and ρ. From these the user can compute additional parameters, such as the percentage of assimilated crust $= \rho / (1 + \rho) * 100$.

For possible publication, 2D Figures can be saved in different formats from R:>file > save as menu, and are written by default into the program directory in EPS format. For 3D figures best results are obtained taking snapshots after manually rotating the graph with the mouse. With windows, the user can do that e.g. with the freeware (for non-commercial use) IrfanView: Options > capture/screenshot > click on the image > file > save image as.

6. Examples of application

In the following we describe the use of AFC3D software for the modelling of some case studies already published in the literature, for

Fig. 4. a) Fig. 1: For AFC non-recharge: r vs ρ plot, derived from Aitcheson and Forrest (1994) Eq. [5].b) Fig. 2: Curves showing the maximum and minimum possible and average values for ρ plotted against r for each element/isotope. It shows the uncertainty given uncertainties in the values of the individual parameters. The possible values are defined by the area where both pairs of maximum and minimum curves overlap. Derived from Aitcheson and Forrest (1994) Eq. [5]. Upper boundaries lacking for most elements, see text for further explanation.c) Fig. 4a: ρ vs r at a fixed β (plotted perpendicular to the β axis). For situations of AFC with recharge, derived from Aitcheson and Forrest (1994) Eqs. [9], [10] and/or [11], d) Fig. 4b: ρ vs β at a fixed r (plotted perpendicular to the r axis). For situations of AFC with recharge, derived from Eqs. [9], [10] and/or [11], e) RGL device 1: 3D graph showing $x = \beta$; $y = \rho$ and $z = r$. This graph shows the surfaces of the different elements (each surface represents an element/isotope ratio) taken into consideration; it is possible to see the set of intersections between them, and to have a first idea about the possible values of the different parameters. In the interactive execution of the program it is possible to rotate the 3D graph with the mouse to observe it from different perspectives, f) RGL device 2: 3D graph showing the curve of intersection of the surfaces. Again, interactive rotation is possible and advisable.

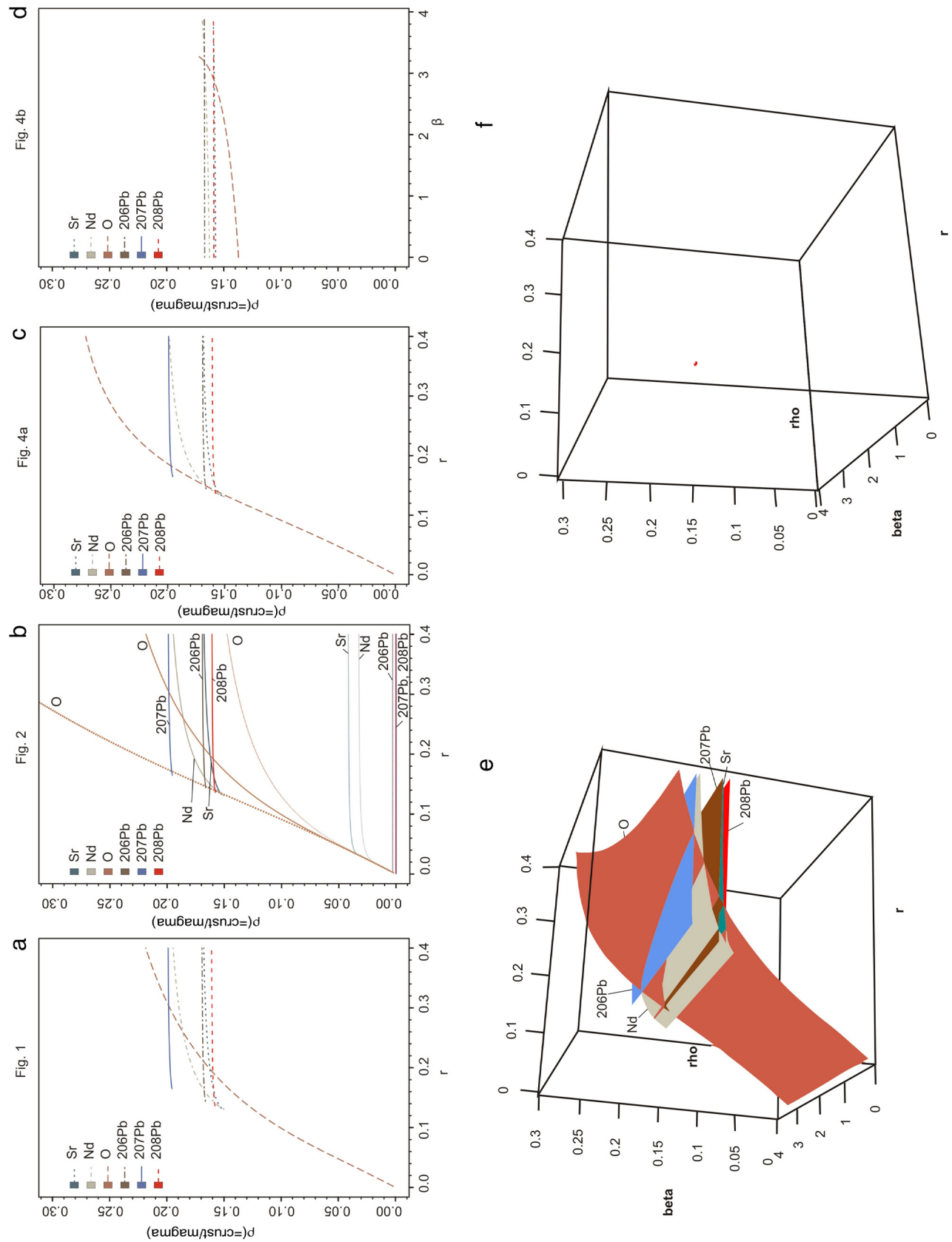
a
Fig. 1
b
Fig. 2
c
Fig. 4a
d
Fig. 4b
e
f
ρ(=crust/magma)
r
β
Sr
Nd
O
206Pb
207Pb
208Pb
207Pb, 208Pb
beta
rho

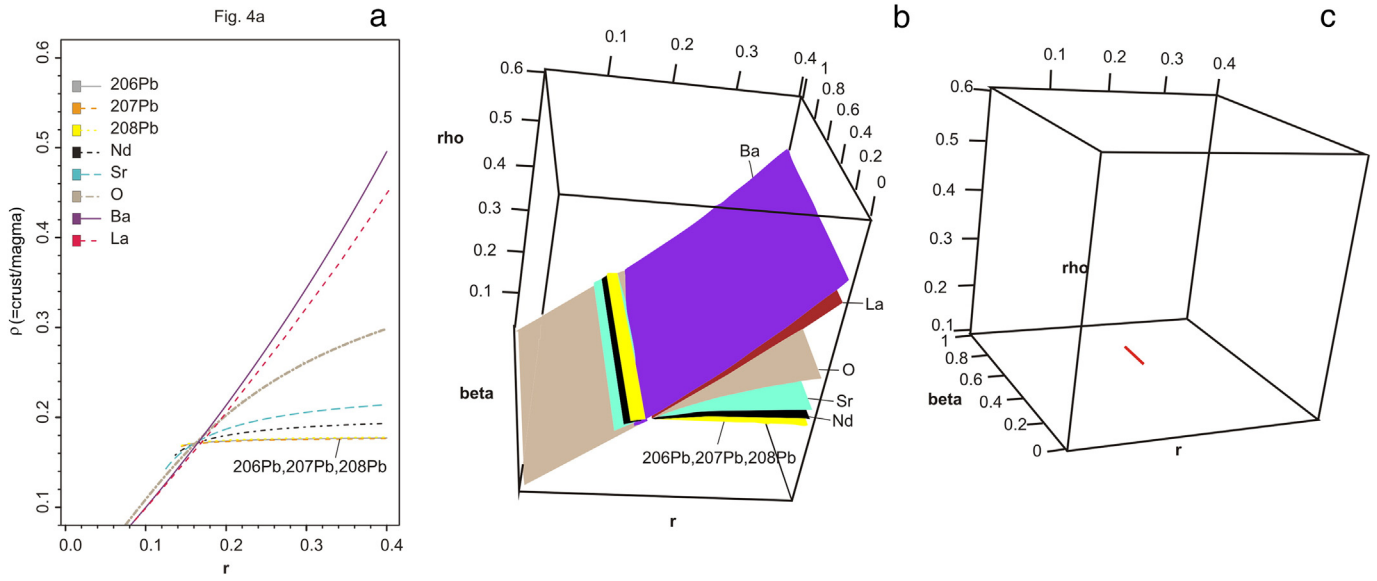

Fig. 5. Output figures from example 1, Taapaca volcano (Wörner et al., 2004). a) r vs ρ, b) RGL device 1: 3D (β, ρ and r) showing surfaces developed by each isotope/element, c) RGL device 2: 3D (β, ρ and r) showing the set of intersections between surfaces developed by each isotope/element.

which we discuss the published solutions and, in some cases, propose additional or alternative ones.

6.1. Example 1. Taapaca volcano, Wörner et al. (2004)

Wörner et al. (2004) used O-, Sr-, Nd- and Pb isotope data to model AFC-r (Aitcheson and Forrest, 1994) for a Taapaca dacite (TAP-002: Mamaní et al., 2010). Their model uses a primitive island arc basalt (Nye and Reid, 1986) as the parent magma and the average of Belen basement (Wörner et al., 2000) as the assimilant. The successful solution predicts $\rho = 0.18$ at an assimilation/fractionation rate of $r = 0.15$. The recharge rate is rather low compared to the assimilation rate ($ß = 0.6$). The authors found the solution consistent with a restricted range of compositions and a long storage and evolution in a thermally buffered magma system. With AFC3D using the isotopes data as in Wörner et al. (2004) and also adding data from two elements (Ba, La) that show similar observed and calculated contents in Wörner's poster, we obtain a similar solution (see Fig. 5): r (~0.17) and ρ (~0.17). Moreover, we show that there is a small influence of the choice of the parameter $ß$, that can be taken as any value between 0.28 and 0.42 without affecting the resulting value of ρ independently of the value of r. Thus the percentage of crustal assimilation is about 15%.

6.2. Example 2. Luingo caldera, Guzmán et al. (2011)

Guzmán et al. (2011) model AFC with recharge using the Las Máquinas basalt (Kay et al., 1999) as the original and recharge magma and the average of selected Ordovician granitoids from the Antofalla Salar (Lucassen et al., 2001) as the contaminant.

The authors selected the theoretical paragenesis of this basalt (Caffe et al., 2002) at 5 kbar and $F = 0.5$ (fraction of magma remaining); i.e., CPx: 67%, Pl: 33%. They used Sr and Nd isotopes data to perform the modeling. Table 7 in Guzmán et al. (2011) presents three possible solutions ($ß$, r, ρ) for the AFC-r using the graphical method proposed by Aitcheson and Forrest (1994). Using zero (i.e., no recharge, solution 1) or low values for $ß$ in the presence of high values of bulk D (i.e., highly compatible elements) can lead to an overestimation of ρ. Therefore, they argued that solutions with higher values of $ß$ (solutions 2 and 3) are more plausible. Considering all the range of possible values of $ß$, they always obtain percentages of crustal melts between 17 and 23%. Fig. 6(a, b) shows that the complete set of solutions using a 1E−3 threshold is much larger, corresponding to the full set of intersections between the surfaces associated to each element/isotope. Moreover, when reducing the threshold to a very low value (19E−6) we find only two possible solutions (Fig. 6c), 1) $r = 0.37$; $\beta = 0.03$ and $\rho = 0.29$ and 2) $r = 0.21$; $\beta = 1.32$ and $\rho = 0.24$ that represent 19.4–22.5% of assimilated crust. As we can see, the percentages of assimilated crust do not vary greatly, but instead the whole set of solutions imply higher differences in the rate of replenishment/rate of assimilation (β) and the rate of assimilation/fractional crystallization (r). These differences are maybe better understood when assessing the relative sizes of rate of assimilation ($\dot{M}_a$): rate of crystallization ($\dot{M}_c$) and rate of replenishment ($\dot{M}_r$). In this case the first solution gives: $\dot{M}_a : \dot{M}_c : \dot{M}_r = 37 : 100 : 1$ and the second solution = 21:100:28.

6.3. Example 3. Northern Puna Magmas, Caffe et al. (2002)

Caffe et al. (2002) modelled AFC processes following Aitcheson and Forrest (1994) for a set of Miocene rocks from the Northern Puna. We choose three of their models to compare with AFC3D, thus including the possibility of AFC-r. Bellow we worked with the data of models A, B and C of that contribution.

6.3.1. Model A (Table 8; Table 11 and Tables B1 and B2 of Appendix B in Caffe et al., 2002)

Their parental magma is the Maquinas basalt (Kay et al., 1999) except for Pb isotopes that were taken from uncontaminated basanites from the Puna. The contaminants are Cretaceous granulitic xenoliths of the Salta Rift (Lucassen et al., 1999) that are representative of the lower crust. We perform the model labelled # Northern Puna magmas_Caffe et al., 2002—Model A # step 1. With AFC3D it is possible to obtain a set of solutions with a threshold of 35E−3 using $^{206}Pb/^{204}Pb$, $^{87}Sr/^{86}Sr$ and εNd isotopes and Ba, Rb and La. However, Figs. 4a and Device 1 highlight that the degree of uncertainty in the r variable is high, so we selected the element that has an intermediate r value plus the isotopes and rerun the AFC3D (labelled #step 2) to obtain a more accurate result; in this step (Step 2) we also change the fixed values of r and β and the extreme values of β. Here we obtain 13 possible

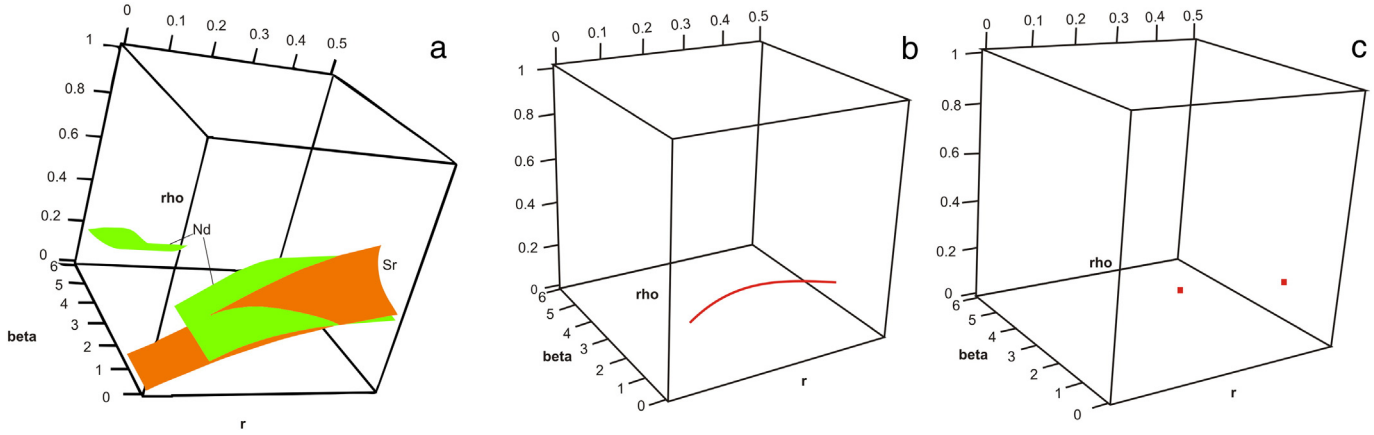

Fig. 6. Output figures from example 2, Luingo caldera (Guzmán et al., 2011). a) RGL device 1: 3D (β, ρ and r) showing surfaces developed by each isotope for solution 3, b) RGL device 2: 3D (β, ρ and r) showing the set of intersections between surfaces developed by each isotope ratio for solution 3, c) RGL device 2: 3D (β, ρ and r) showing the line of intersection between surfaces developed by each isotope ratio, enhancement with lower threshold.

solutions, but if we look at 2D figures, we find out that the Pb isotope does not really intersect the other curves (Fig. 7a), as they have almost parallel profiles. Then, we run a last step (Step 3) with an even lower threshold, and not considering the Pb isotope ratio. In this step, only 3 solutions are possible (see Fig. 7b, c). With a 2E−4 threshold, the resulting r (~0.33) and ρ (~0.28) values are similar to the ones obtained by Caffe et al. (2002) ($r = 0.4$, $\rho = 0.27$–0.33), but with β values between 0.52 and 0.53 (note that although the Pb isotope ratio remains in the figures, as it is a parameter included in the list from the AFC_Input_Data.R file, it is not used for the calculations that lead to find the intersections). We found it interesting that the evaluation of the possibility of recharge should reside mostly in the petrological features that demonstrate its involvement. If we compare Caffe's data with the ones obtained with AFC3D we find out that anyway the crystallization rates and assimilation rates are much higher that the replenishment rates, as our model implies an $\dot{M}_i:\dot{M}_r:\dot{M}_a$ ratio of 33:100:17 for both models are similar: 21–25% for Caffe et al. (2002) and 22% with AFC3D.

6.3.2. Models B and C (Table 8; Table 11; Tables B1 and B2 of Appendix B in Caffe et al., 2002)

They use the Maquinas basalt (original magma) as the mafic member. The global partition coefficients used in models B and C, vary slightly in reason of the different pressure conditions (model B at 7 kbar, Model C at 5 kbar) at the time they use the same contaminant from the medium-upper crust (Puna Paleozoic granitoids, Becchio et al., 1999). In a first step we try to obtain the model with the same input data as in Caffe et al. (2002) using $^{206}Pb/^{204}Pb$, $^{87}Sr/^{86}Sr$ and εNd isotopes and Ba, Rb and La. Using the whole set of data does not lead to a satisfactory result (step 1), however not considering εNd and $^{206}Pb/^{204}Pb$ data, that have curves that are almost parallel to the one of $^{87}Sr/^{86}Sr$, allows finding a set of possible solutions (see Fig. 7d,e,f) with an acceptable threshold value of 2.5E−2.

This model fairly coincides with the one obtained by Caffe et al. (2002). Firstly it allows no recharge as β is in the range of 0–0.2, and secondly, r and ρ have almost the same values. The results obtained by Caffe et al. (2002) are $r = 0.3$ and $\rho = 0.17$–0.21, while those obtained with AFC3D are $r = 0.27$ and $\rho = 0.2$, implying a crustal assimilation of about 17%.

6.4. Additional examples

Additional examples are presented and discussed in detail in Appendix B, in a trial-and-error fashion that allows the reader to repeat the procedure that has to be followed to proceed from an initial rough first guess to the determination of the best set of solutions. Appendix A therefore provides a useful "hands-on" training for the potential user.

7. Results and discussion

The AFC3D software constitutes a helpful tool for modelling AFC and AFC-r processes on the basis of the formulas from DePaolo (1981) and the enhancement of the graphical solution presented by Aitcheson and Forrest (1994). This software provides a graphical 3D representation of ρ as a function of r and β for each element/isotope, thus enabling the user to find, in an easy way, the possible lines/points of intersection that result in a unique solution or a set of solutions. This contribution is intended only as a tool for facilitating the geochemical modelling of assimilation and recharge, but the petrological processes themselves need to be carefully assessed by the user for geological plausibility. Many mathematical solutions can be found, but it is extremely important to check the degree of confidence that the input and output data have.

An important condition that needs to be satisfied to get reliable results is to choose elements/isotope ratios that produce curves with moderate to high intersection angles that in turn are highly dependent on the global partition coefficient (D) of a given element. Evidently this condition is often not satisfied by the whole set of elements present in a set of rocks, thus the user is recommended to search for elements with contrasting D values for modelling.

DePaolo (1981) and Aitcheson and Forrest (1994) equations require D and r to be constant throughout the whole AFC or AFC-r process, but these does not necessarily imply constant rates of assimilation or fractional crystallization (Aitcheson and Forrest, 1994). As was previously pointed out by Aitcheson and Forrest (1994) the equations of the modelling imply an obvious simplification of a geological process, assuming for instance that the magma is homogeneous throughout its evolution. Another important factor to keep in mind is that the diffusivity varies with the properties of each element, so that this could change the estimation of r and ρ. These problems are less evident when considering steady state long lived systems (Aitcheson and Forrest, 1994).

The equations developed by DePaolo (1981, 1985) and Aitcheson and Forrest (1994) differ from the energy constrained AFC (EC-AFC) models of Spera and Bhorson (2001) in the sense that the whole model is interpreted from a different point of view. The DePaolo (1981) and Aitcheson and Forrest (1994) formulations consider only the chemistry and isotopic composition of the whole rock of the assimilant, while the Kds (and ultimately the global partition coefficient D) are controlled only by crystal phases that separate from the parental magma. These models do not consider the thermodynamics of melting, nor the variety of reactions, melt compositions, and solid phases that can occur in the

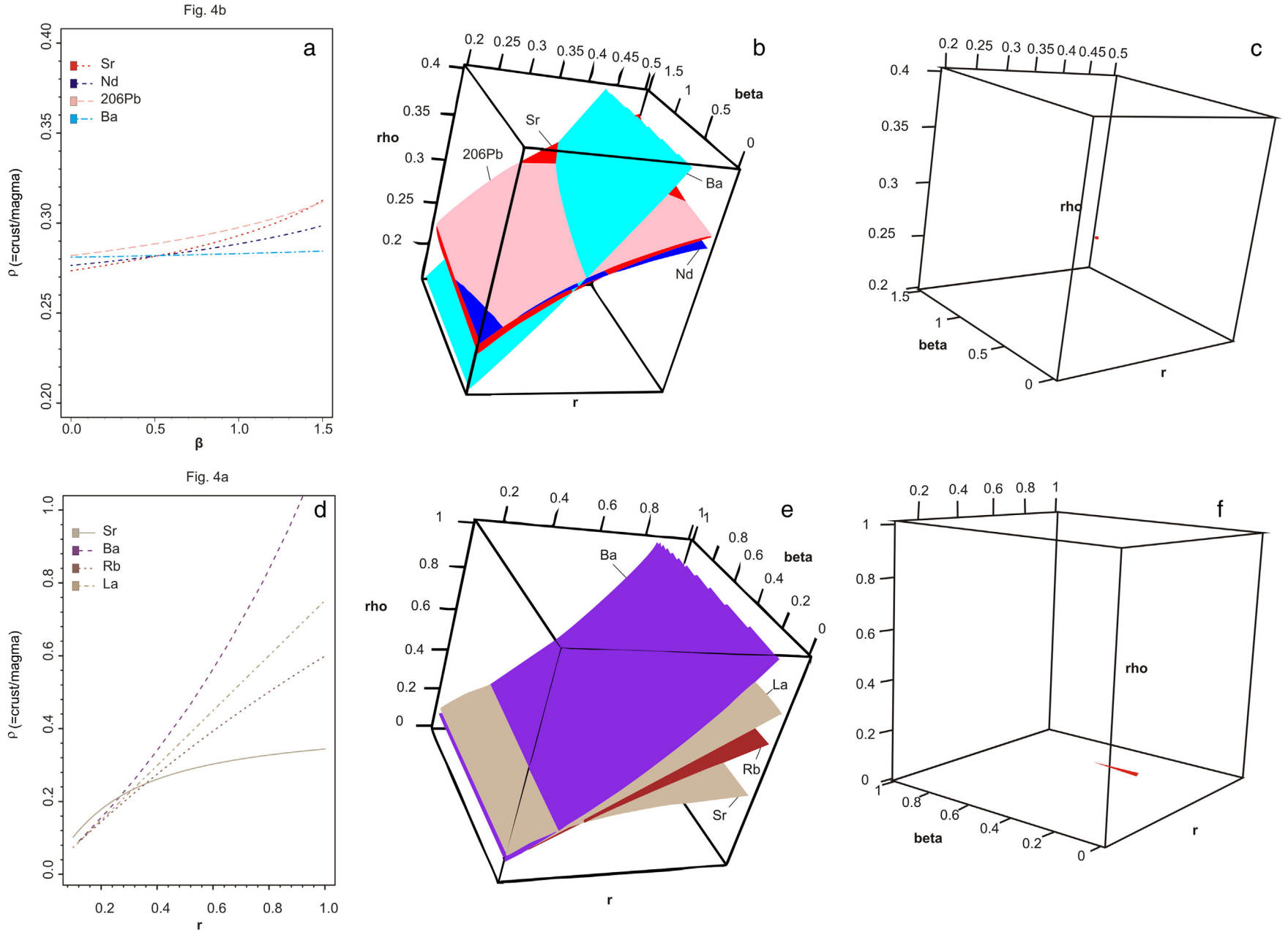

Fig. 7. Output figures from example 3, Northern Puna Magmas_Caffe et al. (2002) a) ρ vs β for model A, note that Pb does not intersect with other elements/isotopes b) RGL device 1: 3D (β, ρ and r) for model A, c) RGL device 2: 3D (β, ρ and r) for model A, d) ρ vs r for models B and C, e) RGL device 1: 3D (β, ρ and r) for models B and C, f) RGL device 2: 3D (β, ρ and r) for models B and C.

contaminant during the progress of assimilation. A comparison between the two methods is not among the objectives of this paper. Nevertheless, the DePaolo (1981) and Aitcheson and Forrest (1994) equations for modelling AFC and AFC-r processes (e.g., Caffe et al., 2002; Guzmán et al., 2011; Kay et al., 2010; Wörner et al., 2004), provide a simpler approach to estimate the amounts of crustal assimilation and rates of crystallization. Considering the uncertainty of assumptions inherent in both models, Caffe et al. (2002) and some of the examples provided in Appendix A show a good agreement between AFC(-R) and EC-AFC, such that conventional AFC models still appear useful and adequate in many cases. Of course, as stated by Caffe et al. (2002) more insights on the hybridization process might be gained from a full EC-AFC treatment, but this would require a better understanding of the composition and thermal state of the crust than is often available. For examples in which the application of the EC-AFC model is difficult due to the lack, or considerable uncertainty, of appropriate data inherent to the model (e.g., melt productivity and extraction of the crustal component, original magma temperature and initial crustal temperature, solidus and liquidus temperatures for the assimilant, etc.) the application of AFC conventional remains simpler and useful and the AFC3D software provides a user-friendly and powerful approach to the exploration of their parameter space.

Acknowledgments

Gerhard Wörner kindly shared with us the geochemical data of Taapaca volcano that were only partially published. The quality of the manuscript was greatly improved by the comments of the Editor-in-chief Andrew Kerr and the comments by Mehmet Keskin, Wendy Bohrson and Glenn Thompson. This work was funded by ANPCyT (PICT 2012-0419; PICT 2011-0407), CONICET (PIP 489) and CIUNSa 2024. The support of the International Cooperation office of CONICET and of CICTERRA-CONICET is also acknowledged.

Appendix A

In the present paper we improve the graphical method developed by Aitcheson and Forrest (1994) on the basis of the DePaolo (1981) and DePaolo (1985) equations. The 3D graphical method presented here not only is able to reproduce the results obtained by Aitcheson and Forrest (1994) but often can allow the researcher to find more accurate solutions with respect to the ones obtained by Aitcheson and Forrest (1994).This is because it allows both graphical and numerical examination of the full set of intersections between two or more surfaces representing, for each element or isotope, the dependence of the parameter ρ as a function of both r and β that can assume simultaneously all the possible values. This is in contrast to the graphical approach of Aitcheson and Forrest (1994), where each of the two parameters could only be varied as the other one was kept fixed at a given value. The user can therefore first determine the complete set of (possibly alternative) solutions, and later discuss and choose, from the full possible set of results, those which guarantee the intersection of a higher number of elements and/or those which appear more plausible from a geological/geochemical perspective.

To illustrate the application of the program we present in the main text of the paper a set of published examples and re-evaluate their results. Moreover, in this appendix we provide additional examples, also taken from the published literature. Some of the examples presented were carried out in situations of recharge, others in no recharge situations. The examples are presented as a trial-and-error procedure, illustrating in practice how to proceed from a rough "first guess" to the final solutions. The objective is to show more accurate or simply alternative possible results from those obtained in the literature. It is very important to highlight however that we will not evaluate in detail the geological plausibility of the different solutions, as this obviously requires a deep knowledge of the geological context related to the data. For a comparison we also present some examples that were modelled in the literature with EC-AFC (Bohrson and Spera, 2001); these examples show that there are cases where the results are roughly comparable, while for other case studies, even using exactly the same input data, the results can be significantly different. This does not immediately imply that one model is better than the other. On the contrary, the choice to use one or the other should be carefully carried out based on the degree of confidence/knowledge of the input data parameters or other reasons that might suggest the choice of the specific model.

Example A

Krienitz et al. (2006) modelled the magma genesis and crustal contamination of Miocene to Quaternary intraplate lavas of northwestern Syria by AFC processes from mantle derived magmas. In particular, they apply EC-AFC modelling obtaining a solution with 25% of continental upper crust assimilation.

Figure 10 of Krienitz et al. (2006) shows that the isotopic and incompatible element variations of the two different Syrian lava groups can be modelled by the EC-AFC processes using two different parental magma compositions. These two parental magmas have approximately similar Sr and Nd isotopic compositions but very different Sr and Nd concentrations, i.e., the high-P group is much more enriched in trace elements than the low-P group lavas. The EC-AFC model indicates that the evolved high-P group lavas have fractionated between 40 and 60% and have assimilated between <5 and about 25% of upper crustal material but suggests higher assimilation rates of up to 45% on the basis of Nd (ppm) versus $^{143}Nd/^{144}Nd$. In contrast, only <10% assimilation and 45–50% fractionation are needed to produce the isotopic composition of the low-P group lavas.

Several modelling attempts were carried out with AFC3D for low-P initial magmas:

1. Trial, step 1 shows possible intersections that lead to models with and without recharge, i.e. β ranging from 0 to 2.86 and very low values of r (0.1 to 0.13) and ρ (0.11 to 0.12).
1. Trial, step 2 better shows the results by reducing the ranges of admissible r (0.01 to 0.6) and β (0 to 1) and also lowering the zero threshold from 1E−2 to 1E−3.

Trial 1, step 3 was carried out reducing even more the ranges for r (0.01 to 0.4) and the zero threshold (1E−4), leading to a set of possible solutions, all of them with recharge.

1. Trial, step 4 was carried out reducing the threshold to a really confident value of 2.8E−6; this gives only two possible results, both of them requiring a recharge situation and a value of $\rho = 0.11$, equivalent to 10% of assimilated crust, in exact coincidence with the results of <10% assimilation published by Krienitz et al. (2006).
2. Trial, step 1 attempts to force a non-recharge situation, but no intersection can be found.
2. Trial, step 2 also requires a non recharge situation, but increasing the zero threshold to 1.4 E−4; this leads to a set of solutions with ρ values of 0.11, thus giving again the same % of crustal assimilation obtained by Krienitz et al. (2006).

For high P initial magmas:

1. Trial, step 1 shows a big set of possible solutions. We begin by modelling with high r, β and ρ ranges, and also a relatively high zero threshold (1E−2). The ranges of solutions are: $r = 0.17$ to 0.29, $\beta = 0$ to 2.35, $\rho = 0.21$ to 0.26.
1. Trial, step 2 reducing all parameters ranges ($r = 0.01$ to 0.5; $\beta = 0$ to 1) and zero threshold = 4E−4, we find a set of solutions with $r = 0.26$ to 0.27, $\beta = 0$ to 0.49 and $\rho = 0.25$ to 0.26

1. Trial, step 3 reducing further the threshold (3.4E−6), two solutions are found: 1) $r = 0.26$, $\beta = 0.31$, $\rho = 0.25$, 2) $r = 0.25$, $\beta = 0.87$, $\rho = 0.25$.
2. Trial, step 1. First attempt to force a non-recharge situation. However, setting a zero threshold of 1E−5 does not lead to any intersections.
2. Trial, step 2. Rising the zero threshold to 1.8E−4 leads to a set of solutions with $r = 0.27$ and $\rho = 0.26$.
In both cases (1.Trial and 2.Trial), recharge and non recharge situations, the solutions that represent the best intersections give crustal assimilation of 20–21%, similar to one of the results proposed by Krienitz et al. (2006). The assimilation rate is of about 27, lower than that obtained by Krienitz et al. (2006) but still, consistently with what was found by the authors, higher than the assimilation rates obtained for low P initial magmas.

Example B

Ma et al. (2013) studied the evolution and origin of the Miocene continental intraplate basalts on the Aleppo Plateau and surrounding areas in NW Syria. The authors divide the Miocene volcanism of the studied area in two phases: ~19–18 Ma (Phase 1-with low trace elements contents) and ~13.5–12 Ma (Phase 2-enriched in trace elements). The authors model AFC processes for the two phases with different parental magmas: for Phase 1 a peridotitic mantle source is used, while for Phase 2, the source is taken as that of amphibole-rich metasomatic veins.

The resulting AFC solutions give a common value $r = 0.6$, while ρ values vary between 27% for Phase 1 and 57% for Phase 2.

In the attempt to reproduce Ma et al. (2013) results with AFC-3D, the 1.Trial and 2.Trial were carried out for Phase 1 magmas (low trace elements contents), finding the following solutions:

1. Trial, step 1: intersection of Nd and Sr isotopes, with wide ranges of r (0–3), β (0–3) and ρ (0 to 3) and with a high threshold value (1E−2). A big set of solutions is found, with preferred results of $r = 0.1$ to 0.18; $\beta = 0$ to 2.68 and $\rho = 0.11$ to 0.13
1.Trial, step 2: reducing all ranges of r (0.02 to 0.2), β (0 to 1), ρ (0.01 to 0.4) and a zero threshold of 8E−5 we find a good intersection with a set of solutions (solution 1) with very low values of $r = 0.13$, β (0 to 0.76) and $\rho = 0.12$. This solution implies about 11% of assimilated crust.
2. Trial, step 1: fixing the r value around 0.6 as in Ma et al. (2013) solution, with a zero threshold of 1E−2, we find no intersection.
2. Trial, step 2: fixing the r value around 0.6 and increasing the zero threshold to a very high value of 2.9E−2, a surface of possible solutions is found. Note that this result is not reliable as the 3D graph shows that there is no real intersection: the surfaces of isotopes are approximately parallel and the result is found only because of the very high value of the zero threshold.
3. Trial and 4.Trial are for Phase 2 magmas (enriched in trace elements); the following solutions are found:
3. Trial, step 1: big ranges of all parameters ($r = 0$ to 3, $\beta = 0$ to 3, $\rho = 0$ to 3) and high zero threshold of 1E−2: two possible surfaces of solutions are found.
3. Trial, step 2: restricting the ranges of r (0 to 0.8) and ρ (0 to 0.5), two possible surfaces of solutions are found, with r ranging from 0.1 to 0.39, $\beta = 0$ to 2.92 and $\rho = 0.29$ to 0.34.
3. Trial, step 3: lowering zero threshold value to 1E−4, still two surfaces of intersection are found.
3. Trial, step 4: further lowering the zero threshold up to 1E−5 we get four solutions: 1) $r = 0.33$ $\beta = 0.24$, $\rho = 0.31$; 2) $r = 0.14$, $\beta = 2.86$, $\rho = 0.35$; 3) $r = 0.10$, $\beta = 2.93$, $\rho = 0.34$; 4) $r = 0.09$, $\beta = 2.94$, $\rho = 0.34$, thus indicating AFC with recharge with crustal assimilation of 23–26%.
4. Trial, step 1: forcing almost a no-recharge situation, i.e. fixing β near zero with high initial zero threshold of 1E−2, we find a big set of solutions.
4. Trial, step 2: reducing zero threshold up to 5E−4, we obtain solutions with $r = 0.33$ and $\rho = 0.31$ for AFC with no recharge.

Our results are fairly different to the ones obtained by Ma et al. (2013) by the Aitcheson and Forrest (1994) method but, on the other hand, they are much more similar to their results by the MELTS program on the basis of major elements variations.

Example C

Schmitt et al., 2006—Geochemistry of volcanic rocks from the Geysers geothermal area, California Coast Ranges.

Schmitt et al. (2006) modelled by AFC dacitic (and rhyolitic) lavas from Cobb Montain, Pine Mountain and Tyler Valley and core samples from the shallow microgranite phase of the GPC, with two end members: (1) coeval basalt of Caldwell Pines (parental magma) that has compositional affinities to magmas extracted from a subcontinental mantle-wedge, and (2) regional crustal rocks equivalent to those of the Franciscan and Great Valley sequence.

The authors perform AFC modelling using Aitcheson and Forrest (1994) formulations and by EC-AFC using the approach of Bohrson and Spera (2001). The authors conclude that the most feasible models from EC-AFC are those modelled under high pressure and high temperatures (models 3, 4 and 5) that lead to (F) values (i.e. mass % of remaining magma) of 20%.

They conclude that calculations at equilibration temperature by Aitcheson and Forrest (1994) give similar results, with mass % of remaining magma relative to the original basalt of ~20%. Their obtained values for AFC without recharge show r values between 0.1 and 0.3, and ρ values between 0.1 and 0.4. The authors also mention possible results that include magma recharge.

We could not reproduce completely the Aitcheson and Forrest AFC-R example as no Oxygen D value is given.

In 1.Trial, all elements and isotopes are used ($^{206}Pb/^{204}Pb$, $^{208}Pb/^{204}Pb$, $^{87}Sr/^{86}Sr$, $^{143}Nd/^{144}Nd$, La, Yb) but no possible intersection is found.

Even in the 2.Trial, where all the isotopes are used, no possible intersection appears.

The 3.Trial includes only three isotopes ($^{208}Pb/^{204}Pb$, $^{87}Sr/^{86}Sr$ and $^{143}Nd/^{144}Nd$). Still no intersection is found.

The 4.Trial examines only 2 isotopes ($^{87}Sr/^{86}Sr$ and $^{143}Nd/^{144}Nd$). This is a recommended procedure as the isotopes not only intersect but also they have an acceptable angle of intersection. In this way we can obtain two possible solutions, with and without recharge, with both solutions giving F values of around 0.5 (i.e. 50% of remaining magma).

In the 5.Trial, other 2 isotopes are used, in this case $^{208}Pb/^{204}Pb$, $^{87}Sr/^{86}Sr$. Also for this trial we obtain at least two possible solutions, with F values of around 0.4.

Without discussing geological plausibility, if one has to decide between trials fourth and fifth only based on the 3D graphical solution, the best solution would probably be the one with $^{208}Pb/^{204}Pb$, $^{87}Sr/^{86}Sr$, because of the requirement of high intersection angle is better satisfied.

Also in the 6.Trial, with 2 isotopes ($^{208}Pb/^{204}Pb$ and $^{143}Nd/^{144}Nd$) a high intersection angle is achieved. The set of solutions give $r = 0.19$, $\beta = 0.14$ to 0.68, and $\rho = 0.23$. However, the resulting F value is particularly low, approximately 0.05, which may be not plausible.

A proper AFC-R modelling should obviously give the same intersection points independently of the chosen (pair of) elements. The fact that choosing different pairs of elements leads to different results implies that the user should choose among several alternatives. This could be done e.g. on the base of the confidence that one puts on the different experimental data. An alternative could be that of determining an

"average" solution for the model parameters. This corresponds in the program to the use of a much higher value for the intersection threshold while looking for the intersection of many (or even all) different elements.

Example D

Goss et al. (2011) modelled the Incapillo Lavas with EC-AFC. The authors use as assimilants Paleozoic granitoids, El Peñon Paleozoic granitoids and average bulk upper crust. The used parental magma is a sample from the Pircas Negras andesite (Goss and Kay, 2009).

In our first attempts to reproduce their model with AFC3D, we used the whole ranges of parameters, including the extreme values of the contaminants, and also the different *D* values that they use in models A to F by EC-AFC. Finally we tried one by one the different models.

The 1.Trial is carried out by trying to intersect all elements and isotopes; this initial trial shows a wide range of input parameters (r, β and ρ all varying from 0 to 3) and a high zero threshold of 1E−2. No intersections are found.

The 2.Trial is with elements only (no isotopes) and with the same parameters ranges and zero threshold as the first trial. No intersections are found.

3. Trial (and following ones) is carried out by observing the 3D graph that helps choosing the possible elements/isotopes that can be intersected. If we choose Ta, Sm and La we find a successful intersection. Solution 1: $r = 0$ to 1.38, $\beta = 0$ to 1.5, $\rho = 0$ to 0.24.

4. Trial is with Yb and La. Solution 2: $r = 0$ to 0.83, $\beta = 0$ to 1.5, $\rho = 0$ to 0.06

5. Trial is Yb, Sm and $^{87}Sr/^{86}Sr$. Solution 3: $r = 0.51$to 0.52, $\beta = 0$ to1.5, $\rho = 0.11$

6. Trial is Eu, Ta, $^{87}Sr/^{86}Sr$. Solution 4: $r = 0.25$ to 0.27, $\beta = 0$–1.0, $\rho = 0.1$

7. Trial is $^{143}Nd/^{144}Nd$ and Th. Solution 5: $r = 0$ to 0.39, $\beta = 0$ to .76, $\rho = 0$ to 0.42

Of all the possible solutions obtained by AFC3D, the ones that give similar results to EC-AFC by Goss et al. (2011) in terms of *r* values are solutions 2, 3 and 5.

Solution 2 is found with Yb and La, that are 2 elements with highly variable *D*, solution 5 ($^{143}Nd/^{144}Nd$, Th) with less contrasting *D* values and solution 3 with approximately similar *D* values. Thus, the potential best solution in the sense of the criterion proposed by Aitcheson and Forrest (1994) is solution 2. Obviously none of these solutions is a "true" solution, as the requisite that all the elements/isotopes intersect is never achieved.

The following trials (8.Trail to 12.Trial) are carried out trying to reproduce models A to F by Goss et al. (2011) individually, but only with isotopes as in Goss et al. (2011). None of these trials leads to a positive result.

Thus the general result is that Goss et al. (2011) provides an interesting example for which the AFC3D modelling cannot provide results that fit the ones obtained by EC-AFC. Once again, this observation does not provide a straightforward evidence that one of the two modelling strategies is better than the other.

Example E

We here perform Model A from Caffe et al. (2002) by EC-AFC. The AFC3D model is presented in the manuscript (see item 6.3.1). The contaminant is represented by granulitic Salta Rift xenoliths and the parental magma is the Maquinas basalt (Kay et al., 1999). Table A1 shows the input parameters.

Basalt T liquidus (1320 °C) in Ni-NiO buffer conditions and the composition of the residual liquid and mineralogical association were obtained by PELE software (Boudreau, 1999); *T liq* was estimated at 10 kbar assuming a slightly thickened crust of 40 km thick for the high lower Miocene in the North Puna. The assimilant *T* liquidus was estimated at 1100 °C as it is a dehydrated granulite (0.5 % H_2O) of granitic composition and by comparison with the curves for granitic melts defined by Holtz et al. (2001). The initial T of the assimilant was recommended by Bohrson and Spera (2001) for contamination at lower crustal levels. The solidus T was estimated from a model of isobaric complete crystallization at 7kbar for the Maquinas basalt by the PELE software (803 °C).

The equilibrium T achieved on EC-AFC for 50 % of crystallization (Mc ~0.5) is of 1137 °C, approximately coincident with the temperature obtained by the PELE software (1170º C) for 50 % of crystallization of the Maquinas basalt at 7 kbar and an andesitic residual liquid composition (57.3 % de SiO_2). Note that in the isobaric crystallization model done by PELE there is no loss of T introduced by the colder contaminant (600 °C).

Cpm and *Cpa* (specific heat of pristine magma and assimilant respectively) were obtained from the chemical composition of the basalt and the xenolith SR 4-304a of Lucassen et al. (1999), and from the reference values for each oxide from Table 3 in Spera and Bohrson (2001). Values of *hcry* (crystallization latent heat) and *hfus* (fusion heat) were taken from the standard case of contamination in lower crust of Table 1 in Bohrson and Spera (2001).

The productivity of the melt was estimated with a non linear function, within the ranges of values (a and b) suggested by Bohrson and Spera (2007), from estimations for melt and assimilant done with PELE software and making sure that the resulting curves converge in 1 and 0, i.e., in the liquidus and solidus respectively.

Table A1
Input parameters for Example E.

Equilibration parameters		Tl,m	1320	degC	Magma a	900	Element	Sr	Nd	Ba	Rb	La
Teq Norm	0.885	T°m	1320	degC	Magma b	−10.5	Magma:conc.	500	16	208	25	11
Teq deg C	1136.787	Tl,a	1100	degC	Assimilant a	400	Bulk D0	1.14	0.69	0.12	0.07	0.17
Mm	0.914754	T°a	600	degC	Assimilant b	−11	Enthalpy	0	0	0	0	0
M°a	0.415948	ts	800	degC			Assimilant: conc.	300	38	526	21	45
Ma*	0.415228	Cp,m	1434	J/Kg K			BulkD0	1	1	0.12	0.07	0.17
Mc	0.500474	Cp,a	1406	J/Kg K			Enthapy	0	0	0	0	0
fa	0.998269	Hcry	396,000	J/Kg			Isotope	$^{87}Sr/^{86}Sr$	$^{143}Nd/^{144}Nd$			
fm	0.499526	Hfus	354,000	J/Kg			Ratio magma	0.704	0.5128			
M°a/Mc	0.831108						Ratio assimilant	0.715	0.51211			

Teq norm: normalized equilibration temperature of system; Teq deg C: equilibration temperature; Mm: mass of melt in magma body; M°a: mass of country rock involved in RAFC event; M*a: mass of anatectic melt; Mc: mass of cumulates (normalized to original mass of magma body); fa(T): melt productivity of wall-rock composition; fm(T): melt productivity of pristine initial host melt composition; Tl,m: pristine host melt liquidus temperature; T°m: initial host melt temperature; T l,a: wall-rock liquidus temperature; T°a: initial country rock temperature; Ts: solidus temperature; Cp,m: magma isobaric specific heat capacity; Cp,a: assimilant isobaric specific heat capacity; Hcry: heat of crystallization; and Hfus: heat of fusion.

Table A2
Results from example E: model A from Caffe et al. (2002) by EC-AFC.

Norm T magma	T magma (deg C)	Norm T assim	T assim (deg C)	Mm	fa	Ma*	fm	Mc
0.8850	1136.79	0.8270	1044.38	0.919	0.951	0.396	0.5	0.5
Ma*/Mc	dMa*/dMc	Sr	$^{87}Sr/^{86}Sr$	Nd	$^{143}Nd/^{144}Nd$	Ba	Rb	La
0.791	1.507	402.968	0.70686	26.474	0.512425	439.993	35.449	30.125

Symbols as in Table A1.

The isotopic values for pristine magma and assimilant were taken from Model A in Caffe et al. (2002). *D* values are from the calculated average in Caffe et al. (2002) for the Maquinas basalt at 7 kbar and $F = 0.5$, except for Rb (ppm) and Ba (ppm), where the corresponding values at $F = 0.6$ were chosen. For La (ppm) the average *D* from both models in Caffe et al. (2002) were taken. The *D* for assimilants was fixed at 1 (compatible) for Sr and Nd by means of plagioclase stability at 7 kbar and ~0 % H_2O and the accessory phases that control Nd (zircon, apatite). Rb, even scarce, is highly incompatible given that in granulites from the lower crust there is no biotite. Ba is more abundant, and probably controlled mostly by the K-feldspar. La is considered perfectly incompatible in both the assimilant and in the pristine magma. With all these considerations, Caffe et al. (2002) model A is reproduced by EC-AFC by the thermal and chemical analyses in Table A2.

The results show a good fit for the $^{87}Sr/^{86}Sr$, $^{143}Nd/^{144}Nd$, Sr and Nd (ppm) and for the Ba and La (ppm) and a bad result (very low) for the Rb (ppm).

From the point of view of the generated mass of crystalline cumulates these reach 50 % of M_o and the quantity of melt given by the assimilant is ~40 %, i.e. in the sense of Aitcheson and Forrest (1994) the effective crustal contamination is ca. 28 %.

Model A of Caffe et al. (2002) with AFC-3D reaches a 22% of contamination and the results in Caffe et al. (2002) by AFC "2D" vary between 21 and 25%, without recharge. Hence, given the uncertainties in the all the modelling methods, the results are fairly consistent.

References

Adler, D., Murdoch, D., 2012. rgl: 3D visualization device system (OpenGL). R package version 0.92.880. http://CRAN.R-project.org/package=rgl.

Aitcheson, S.J., Forrest, A.H., 1994. Quantification of crustal contamination in open magmatic systems. Journal of Petrology 35, 461–488.

Becchio, R., Lucassen, F., Kasemann, S., Franz, G., Viramonte, J., 1999. Geoquímica y sistemática isotópica de rocas metamórficas del Paleozoico interior: Noroeste de Argentina y Norte de Chile (21–27°S). Acta Geologica Hispánica 34, 273–299.

Bohrson, W.A., Spera, F.J., 2001. Energy-constrained open-system magmatic processes. II. Application of energy-constrained assimilation–fractional crystallization (EC-AFC) model to magmatic systems. Journal of Petrology 42 (5), 1019–1041.

Bohrson, W., Spera, F., 2007. Energy-constrained recharge, assimilation, and fractional crystallization (EC-RAXFC): a visual basic computer code for calculating trace element and isotope variations or open-system magmatic systems. Geochemistry, Geophysics, Geosystems 8 (11).

Boudreau, A.E., 1999. PELE: a version of the MELTS software program for the PC platform. Computers and Geosciences 25, 201–203.

Bowen, N.L., 1928. The Evolution of the Igneous Rocks. Princeton University Press, Princeton NJ.

Caffe, P.J., Trumbull, R.B., Coira, B.L., Romer, R.L., 2002. Petrogenesis of early volcanic phases in Northern Puna Cenozoic magmatism. Implications for magma genesis and crustal processes in the Central Andean Plateau. Journal of Petrology 43, 907–942.

DePaolo, D.J., 1981. Trace element and isotopic effects of combined wallrock assimilation and fraccional crystallization. Earth and Planetary Science Letters 53, 189–202.

DePaolo, D.J., 1985. Isotopic studies of processes in mafic magma chambers: I. The Kiglapait intrusion, Labrador. Journal of Petrology 26, 925–951.

Goss, A.R., Kay, S.M., 2009. Extreme high field strength element (HFSE) depletion and near-chondritic Nb/Ta ratios in Central Andean adakite-like lavas (28 S, 68 W). Earth and Planetary Science Letters 279 (1–2), 97–109.

Goss, A.R., Kay, S.M., Mpodozis, C., 2011. The geochemistry of a dying continental arc: the Incapillo Caldera and Dome Complex of the southernmost Central Andean Volcanic Zone (28S). Contributions to Mineralogy and Petrology 161, 101–128.

Guzmán, S., Petrinovic, I., Brod, A., Hongn, F., Seggiaro, R., Montero, C., Carniel, R., Dantas, E., Sudo, M., 2011. Petrology of the Luingo caldera (SE margin of the Puna plateau): a middle Miocene window of the arc–back arc configuration. Journal of Volcanology and Geothermal Research 200, 171–191.

Harrell, F.E., 2012. Hmisc: Harrell Miscellaneous. R package version 3.9-3. http://CRAN.R-project.org/package=Hmisc.

Holtz, F., Johannes, W., Tamic, N., Behrens, H., 2001. Maximum and minimum water contents of granitic melts: a re-examination and implications. Lithos 56, 1–14.

Kay, S.M., Mpodozis, C., Coira, B., 1999. Neogene magmatism, tectonism, and mineral deposits of the Central Andes 22° to 33°S latitude. In: Skinner, B.J. (Ed.), Geology and Ore Deposits of the Central Andes. Society of Economic Geologists Special Publication, 7, pp. 27–59.

Kay, S.M., Coira, B., Caffe, P.J., Chen, C., 2010. Regional chemical diversity, crustal and mantle sources and evolution of central Andean Puna plateau ignimbrites. Journal of Volcanology and Geothermal Research 198, 81–111.

Krientiz, M.-S., Haase, K.M., Mezger, K., Eckardt, V., Shaikh-Mashail, M.A., 2006. Magma genesis and crustal contamination of continental intraplate lavas in northwestern Syria. Contributions to Mineralogy and Petrology 151, 698–716.

Lucassen, F., Lewerenz, S., Franz, G., Viramonte, J., Mezger, K., 1999. Metamorphism, isotopic ages and composition of lower crustal granulite xenoliths from the Cretaceous Salta rift, Argentina. Contributions to Mineralogy and Petrology 134, 325–341.

Lucassen, F., Becchio, R., Harmon, R., Kasemann, S., Franz, G., Trumbull, R., Wilke, H., Romer, R., Dulski, P., 2001. Composition and density model of the continental crust at an active continental margin—the Central Andes between 21° and 27° S. Tectonophysics 341, 195–223.

Ma, G.S.-K., Malpas, J., Suzuki, K., Lo, C.-H, Wang, K.-L., Iizuka, Y., Xenophontos, C., 2013. Evolution and origin of the Miocene intraplate basalts on the Aleppo Plateau, NW Syria. Chemical Geology 335, 149–171.

Mamaní, M., Wörner, G., Sempere, T., 2010. Geochemical variations in igneous rocks of the Central Andean orocline (13 S to 18 S): Tracing crustal thickening and magma generation through time and space. Geological Society of America Bulletin 122 (1–2), 162–182.

Nye, C.J., Reid, M.R., 1986. Geochemistry of primary and least fractionated lavas from Okmok volcano, Central Aleutions: implications for arc magmagenesis. Journal of Geophysical Research 91 (B10), 10271–10287.

O'Hara, M.J., 1977. Geochemical evolution during fractional crystallisation of periodically refilled magma chamber. Nature 266, 503–507.

R Development Core Team, 2012. R: A Language and Environment for Statistical Computing. R Foundation, Austria (3-900051-07-0 (www.R-project.org)).

Reagan, M.K., Gill, J.B., Malavassi, E., García, M.O., 1987. Changes in magma composition at Arenal volcano, Costa Rica, 1968–1985: real-time monitoring of open-system differentiation. Bulletin of Volcanology 49, 415–434.

Roberts, M.P., Clemens, J.D., 1995. Feasibility of AFC models for the petrogenesis of calc-alkaline magma series. Contributions to Mineralogy and Petrology 121, 139–147.

Schmitt, A.K., Romer, R.L., Stimac, J.A., 2006. Geochemistry of volcanic rocks from the Geysers geothermal area, California Coast Ranges. Lithos 87, 80–103.

Spera, F.J., Bohrson, W.A., 2001. Energy-constrained open-system magmatic processes I: general model and energy-constrained assimilation and fractional crystallization (EC-AFC) formulation. Journal of Petrology 42 (5), 999–1018.

Wörner, G., Lezaun, J., Beck, A., Heber, V., Lucassen, F., Zinngrebe, E., Rössling, R., Wilke, H.G., 2000. Precambrian and Early Paleozoic evolution of the Andean basement at Belen (northern Chile) and Cerro Uyarani (western Bolivia Altiplano). Journal of South American Earth Sciences 13 (8), 717–737.

Wörner, G., Wegner, W., Kiebala, A., Singer, B., Heumann, A., Hora, J., 2004. Evolution of Taapaca Volcano, N. Chile, Evidence from Major and Trace Elements, Sr-, Nd-, Pb-, and U-series Isotopes, Age Dating and Chemical Zoning in Sanidine Megacrysts. IAVCEI General Assembly, Pucón, Chile.